The electron *g* factor of cylindrical GaAs–$Ga_{1-x}Al_xAs$ quantum well wires under magnetic fields applied along the wire axis

2008 J. Phys.: Condens. Matter 20 175204

(http://iopscience.iop.org/0953-8984/20/17/175204)

J. Phys.: Condens. Matter **20** (2008) 175204 (6pp) doi:10.1088/0953-8984/20/17/175204

The electron g factor of cylindrical GaAs–$Ga_{1-x}Al_xAs$ quantum well wires under magnetic fields applied along the wire axis

F E López[1], B A Rodríguez[1], E Reyes-Gómez[1] and L E Oliveira[2]

[1] Instituto de Física, Universidad de Antioquia, AA 1226, Medellín, Colombia
[2] Instituto de Física, Unicamp, CP 6165, Campinas, São Paulo, 13083-970, Brazil

Received 28 January 2008, in final form 22 February 2008
Published 3 April 2008
Online at stacks.iop.org/JPhysCM/20/175204

Abstract

The effects of confinement and magnetic fields on the effective electron Landé g factor of GaAs–$Ga_{1-x}Al_xAs$ cylindrical quantum well wires are studied. Calculations were carried out via the Ogg–McCombe effective Hamiltonian which is used to describe the non-parabolicity and anisotropy effects on the electron states in the conduction band. The applied magnetic field is taken along the wire axis, and the Schrödinger equation corresponding to electron spin projections parallel and antiparallel to the magnetic field is solved by using an expansion of the electron wavefunctions in terms of two-dimensional harmonic oscillator wavefunctions. Calculations for the electron $g_{\|}$ factor in GaAs–$Ga_{1-x}Al_xAs$ cylindrical quantum well wires are compared with results from previous theoretical work. Moreover, the present results clearly indicate the importance of taking into account the non-parabolicity/anisotropy of the conduction band if one is interested in a quantitative understanding of the electron g factor in GaAs–$Ga_{1-x}Al_xAs$ quantum well wires.

1. Introduction

The study of the interaction between single-particle spins and the solid-state environment has been the subject of a considerable amount of work in the last few years. In particular, studies on the properties of the electron g factor for semiconductor bulk materials [1], quantum wells (QWs) [2–4], quantum well wires (QWWs) [5, 6], quantum dots (QDs) [7], and superlattices (SLs) [8] have attracted the community's attention both from the theoretical and experimental points of view, due to the potential applications in spintronics and optoelectronic devices [9]. In semiconductors and its heterostructures, the effective g factor determines the spin splitting of carrier bands and, therefore, influences the spin dynamics and spin resonance of such materials. Also, manipulation of the electron spin may be used in so-called spin-based electronics, where preservation of the electron spin coherence is required [9]. On the other hand, the electron g factor is very important in the understanding of the physical properties of a two-dimensional electron gas (2DEG), in which the quantum Hall effect (QHE) is observed. For example, in a 2DEG the spin gap is much larger than the single-particle Zeeman energy which may be understood in terms of the enhanced effective g factor due to the electron–electron exchange interaction [10]. In addition, the fractional QHE was studied in the limit of zero g factor [11] in an effort to find large distortions of the spin field including many flipped spins (skyrmions) which are expected to be important in the weak magnetic field limit. The zero g factor of the sample may be tuned, for example, by the application of hydrostatic pressure [12].

Investigations on the properties of the effective Landé g factor have been carried out mainly for QWs and QDs, whereas the case of QWWs has received much less attention. QWWs have proven to be of great value in the active development of electronic and optoelectronic devices, such as nanowire field-effect transistors, crossed, axial, and radial nanowire heterostructures, and so on [13]. Most relevant for the present work is the theoretical study reported by Kiselev *et al* [5], who developed a theory of the Zeeman effect for electrons in one- and zero-dimensional semiconductor systems by using an 8×8 Kane model, and investigated the properties of the electron g factor in QWWs and QDs in the absence of magnetic fields.

The aim of the present work is to study the effects of confinement and magnetic fields on the effective electron Landé g factor in GaAs–$Ga_{1-x}Al_xAs$ cylindrical quantum well wires by using the Ogg–McCombe effective Hamiltonian [14], which takes into account the non-parabolicity and anisotropy effects on the electron states in the conduction band. Section 2 describes the present theoretical framework, in which we study the motion of a conduction electron in a QWW under a magnetic field applied along the wire axis and propose an expression for evaluating the effective Landé factor of such a system. Section 3 is concerned with the present theoretical results and discussion. Conclusions are given in section 4.

2. Theoretical framework

In order to study the confinement and magnetic field effects on the electron g factor for GaAs–$Ga_{1-x}Al_xAs$ QWWs under magnetic fields applied along the wire axis (z direction), we assume the effective mass approximation and take into account the non-parabolicity and anisotropy of the conduction band via the Ogg–McCombe effective Hamiltonian [14], i.e.,

$$\begin{aligned}\hat{H} = {} & \frac{\hbar^2}{2}\hat{\vec{\mathbf{K}}}\frac{1}{m(x,y)}\hat{\vec{\mathbf{K}}} + \frac{1}{2}g(x,y)\mu_{\mathrm{B}}B\hat{\sigma}_z + a_1\hat{K}^4 + \frac{a_2}{l_B^4} \\ & + a_3\left(\left[\hat{K}_x^2,\hat{K}_y^2\right]_+ + \left[\hat{K}_y^2,\hat{K}_z^2\right]_+ + \left[\hat{K}_z^2,\hat{K}_x^2\right]_+\right) \\ & + a_4B\hat{K}^2\hat{\sigma}_z + a_5B\left[\hat{\vec{\sigma}}\cdot\hat{\vec{\mathbf{K}}},\hat{K}_z\right]_+ + a_6B\hat{\sigma}_z\hat{K}_z^2 \\ & + V(x,y). \end{aligned} \tag{1}$$

In the above expression, $\hat{\vec{\mathbf{K}}} = -\mathrm{i}\nabla + \frac{e}{\hbar c}\hat{\vec{\mathbf{A}}}$, $\hat{\vec{\sigma}}$ is a vector whose components are the Pauli matrices, l_B is the Landau length, and $m(x,y)$ and $g(x,y)$ are the position-dependent effective mass and Landé g factor, respectively [15], corresponding to the two different building materials forming the QWW. The height of the electron confining potential $V(x,y)$ was taken as the 60% of the band-gap difference between $Ga_{1-x}Al_xAs$ and GaAs. The coefficients a_1, a_2, a_3, a_4, a_5, and a_6 are constants obtained by a fitting of magnetospectroscopic measurements for bulk GaAs [16][3]. As pointed out by Golubev *et al* [16], the terms proportional to a_1 and a_3 in the Ogg–McCombe effective Hamiltonian govern the energy dependence of the cyclotron effective mass. The term proportional to a_2 gives the diamagnetic shift of the Landau electronic levels, whereas the spin-dependent terms, proportional to a_4, a_5, and a_6, contribute to changes in the electron Landé factor of the heterostructure. To our knowledge, [16] is the only work in which values of the coefficients a_i ($i = 1, 2, \ldots, 6$) were reported via experimental measurements. Other authors have also used the same coefficients in order to study the magnetic field dependence of the electron spin relaxation in n-type semiconductors [17]. The values of a_i ($i = 1, 2, \ldots, 6$) were considered as the same in the well and barrier materials[3].

[3] We have used the values $(a_1, a_2, a_3) = (-2.9, -2.6, -1.2) \times 10^6$ meV Å^4 and $(a_4, a_5, a_6) = (9.7, -0.8, 4.9)$ meV Å^2 T^{-1} in the present theoretical calculations.

The wavefunctions of (1) may be chosen as

$$\Psi_j(\vec{\mathbf{r}}) = \begin{pmatrix}\psi_{j,\uparrow}(\vec{\rho}) \\ \\ \psi_{j,\downarrow}(\vec{\rho})\end{pmatrix}\mathrm{e}^{\mathrm{i}k_z z}, \tag{2}$$

where $\vec{\rho} = (x, y)$, k_z is the electron wavevector along the wire axis and ψ_{j,m_s} the electron wavefunctions in the plane perpendicular to the wire axis for a given value of the m_s projection ($\uparrow$ or $\downarrow$) of the electron spin along the magnetic field direction. Here we have taken $k_z = 0$, which corresponds to focusing on the lowest quasi-one-dimensional (wire) conduction electron subband edge. Such approximation was successfully used in the study of the effective Landé factor for semiconductor QWs [4] at low temperatures and very low electron densities, so many-particle effects in the conduction band may be disregarded and a one-electron Hamiltonian may be used to describe the conduction electron states. The Hamiltonian (1) then becomes diagonal and the $\uparrow$ spin-up and $\downarrow$ spin-down states are uncoupled. The Schrödinger equation is therefore given by

$$\begin{pmatrix}\hat{H}_\uparrow & 0 \\ \\ 0 & \hat{H}_\downarrow\end{pmatrix}\begin{pmatrix}\psi_{j,\uparrow}(\vec{\rho}) \\ \\ \psi_{j,\downarrow}(\vec{\rho})\end{pmatrix} = E\begin{pmatrix}\psi_{j,\uparrow}(\vec{\rho}) \\ \\ \psi_{j,\downarrow}(\vec{\rho})\end{pmatrix}, \tag{3}$$

where $\hat{H}_\uparrow$ and $\hat{H}_\downarrow$ describe the spin-up and spin-down electron states, respectively, and are obtained from the $k_z = 0$ diagonal components of (1). The vector potential may be chosen as $\vec{\mathbf{A}} = \frac{1}{2}\vec{\mathbf{B}} \times \vec{\mathbf{r}}$ and the wavefunctions ψ_{j,m_s} expanded in terms of the two-dimensional harmonic oscillator eigenfunctions written in polar coordinates, i.e.,

$$\psi_{j,m_s}(\vec{\rho}) = \sum_k C_{jk}(m_s)\phi_k(\vec{\rho}), \tag{4}$$

$$\phi_k(\vec{\rho}) = A_{n_k,l_k}\left[\frac{\rho}{\sqrt{2}l_B}\right]^{|l_k|}\mathrm{L}_{n_k}^{|l_k|}\left(\frac{\rho^2}{2l_B^2}\right)\mathrm{e}^{-\frac{\rho^2}{4l_B^2}+\mathrm{i}\theta l_k}, \tag{5}$$

where $A_{n_k,l_k} = [\frac{n_k!}{2\pi l_B^2(n_k+|l_k|)!}]^{\frac{1}{2}}$ and $\mathrm{L}_{n_k}^{|l_k|}$ are the associated Laguerre polynomials. Expansion (4) may be used to write the Hamiltonian $\hat{H}_{m_s}$ in the harmonic oscillator representation, with corresponding eigenvalues obtained by solving the algebraic problem

$$\sum_k\left[H_{m_s}^{jk} - E_n(m_s)\delta_{jk}\right]C_{nk}(m_s) = 0, \tag{6}$$

where $H_{m_s}^{jk} = \langle\phi_k(\vec{\rho})|\hat{H}_{m_s}|\phi_j(\vec{\rho})\rangle$ and k correspond to radial and magnetic quantum numbers, i.e., $k \equiv (n_k, l_k)$ (see the appendix for details). Here, we are particularly interested in the electron g factor associated with the ground state $\uparrow$ and $\downarrow$ energy levels, i.e.,

$$g_\parallel = \frac{E_0(\uparrow) - E_0(\downarrow)}{\mu_{\mathrm{B}}B}, \tag{7}$$

where μ_{B} is the Bohr magneton. Note that the above expression, which defines the effective electron Landé $g_\parallel$ factor in the wire axis direction, is a consequence of the decoupling of the spin-up and spin-down electron states in the $k_z = 0$ approximation, and that $g_\parallel$ may be a function both of the applied magnetic field and structural parameters of the wire.

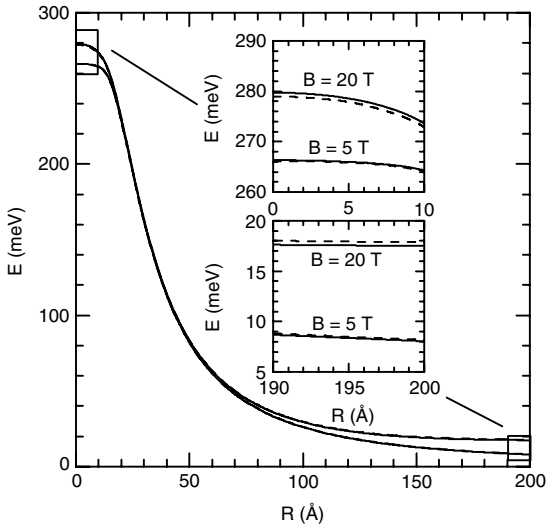

Figure 1. Electron energy associated with the bottom ($k_z = 0$) of the first conduction electron subband, for spin-up (solid lines) and spin-down (dashed lines) states in GaAs–$Ga_{0.65}Al_{0.35}As$ cylindrical QWWs as a function of the wire radius. Calculations were performed for $B = 5$ T and $B = 20$ T.

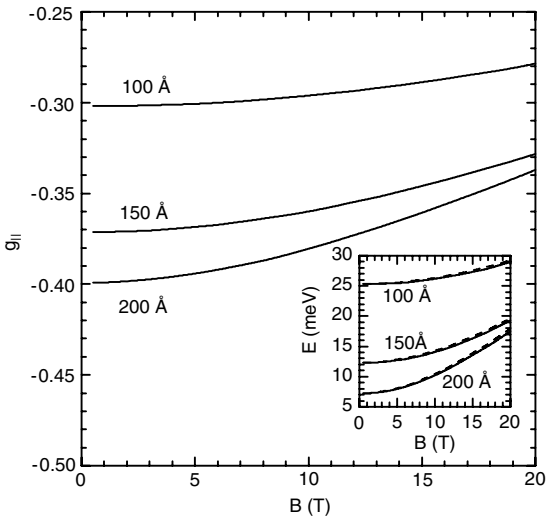

Figure 2. Magnetic-field dependence on the electron $g_{\|}$ factor for GaAs–$Ga_{0.65}Al_{0.35}As$ cylindrical QWWs in three different values of the wire radius. Ground state energies for spin-up (solid lines) and spin-down (dashed lines) states are also displayed in the inset.

3. Results and discussion

In the present work we have focused on GaAs–$Ga_{1-x}Al_xAs$ cylindrical QWWs, with Al proportion $x = 0.35$, under magnetic fields applied along the wire axis. Figure 1 displays the electron energies corresponding to the first conduction electron subband at $k_z = 0$, as functions of the wire radius, and associated with the electron spin orientations parallel and antiparallel to the magnetic field. Calculations were carried out for two different values of the applied magnetic field. One may notice that, for the lowest values of the wire radius, the spin-up energy is slightly higher than the spin-down energy. On the other hand, for the larger values of the wire radius considered in the calculations, the spin-down energy is higher than the spin-up energy. This behavior is due to a change in the sign of the effective $g_{\|}$ factor, as detailed below.

The electron spin splitting is more remarkable at large values of the magnetic field. In figure 2 we show the magnetic-field dependence of the electron $g_{\|}$ factor in GaAs–$Ga_{0.65}Al_{0.35}As$ cylindrical QWWs for three different values of the wire radius. The corresponding spin-up and spin-down electron energies are also displayed in the inset. The behaviors of the electron energy, for a given projection of the electron spin, result from a competition between the magnetic field and QWW barrier-potential confining effects on the electron wavefunction. Of course, the electron energy decreases as the wire radius is increased due to the decrease in the confinement caused by the wire potential. On the other hand, the electron energy increases with the strength of the magnetic field, due to the increase in the wavefunction localization induced by the applied magnetic field. One may expect, therefore, an effective $g_{\|}$ factor dependent on both the QWW radius and the applied magnetic field (cf figure 2). Moreover, one may note from figure 2 that the effective $g_{\|}$ factor is essentially independent of the magnetic field in the low magnetic field limit, whereas it increases as the magnetic field is increased. It is apparent from figure 3 that the effective $g_{\|}$ factor changes its sign at a certain value of the QWW radius, as the electron g factor for the GaAs well is negative whereas it is positive for the $Ga_{0.65}Al_{0.35}As$ barrier. For a given value of the applied magnetic field and for a sufficiently small value of the wire radius ($R < l_B$), the ground state electron wavefunction penetrates the barrier material, and therefore the effective $g_{\|}$ factor is positive. On the other hand, when the wire radius increases, the wavefunction becomes more localized in the well material and, as a consequence, the effective electron

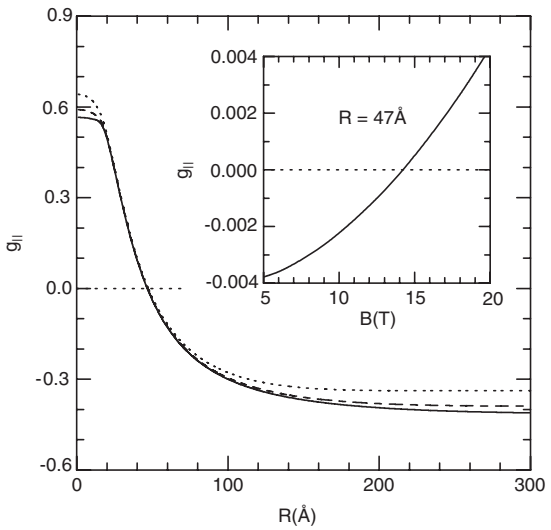

Figure 3. Electron Landé $g_{\|}$ factor of GaAs–$Ga_{0.65}Al_{0.35}As$ QWWs as a function of the wire radius. Solid, dashed and dotted lines correspond to $B = 5$ T, 10 T, and 20 T, respectively. The inset shows the magnetic-field dependence of the $g_{\|}$ factor in a 47 Å width GaAs–$Ga_{0.75}Al_{0.25}As$ QWW.

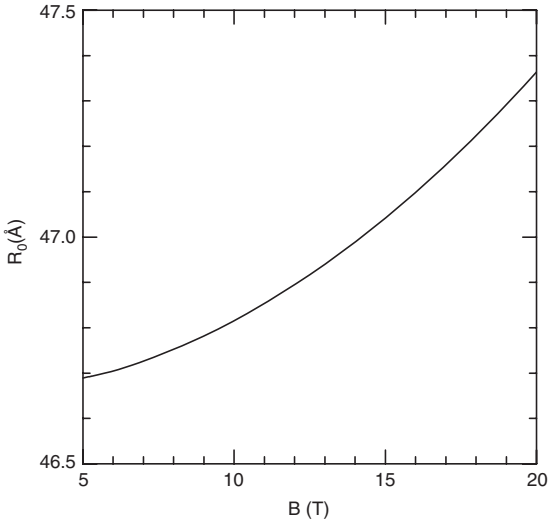

Figure 4. Magnetic-field dependence of the QWW radius for which the electron Landé $g_\parallel$ factor vanishes.

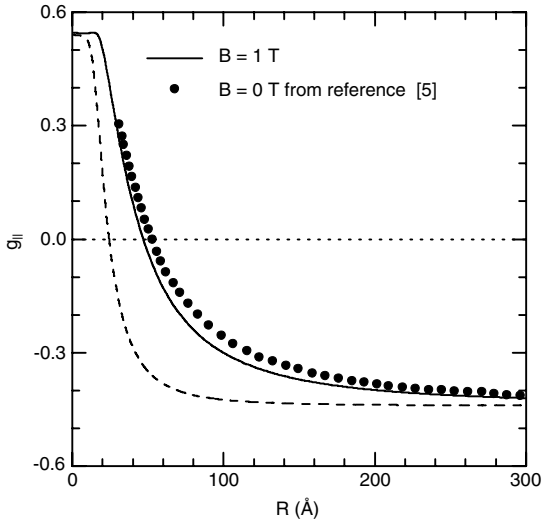

Figure 5. Electron Landé $g_\parallel$ factor as a function of the wire radius for GaAs–$Ga_{0.65}Al_{0.35}As$ QWWs for $B = 1$ T (solid line). The $B = 1$ T dashed line is obtained by disregarding the non-parabolicity/anisotropy contributions ($a_i = 0$ in equation (1)). Solid circles show the numerical results reported by Kiselev *et al* [5].

$g_\parallel$ factor diminishes until it reaches the -0.44 GaAs limiting value for a large wire radius. Thus, the electron $g_\parallel$ factor may be manipulated by changing the geometrical configuration of the wire. In addition, the sign of the effective $g_\parallel$ factor may be changed by the applied magnetic field, as we have shown in the inset of figure 3. The wire radius R_0 for which the electron $g_\parallel$ factor is zero is expected to be a function of the applied magnetic field. Present calculations for R_0 are displayed in figure 4, and are found in good agreement with the numerical result reported by Kiselev and co-workers [5] who obtained this value at about 50 Å.

In figure 5, the present theoretical results for the electron $g_\parallel$ factor at $B = 1$ T, as functions of the wire radius, are compared with the numerical data reported in [5] for GaAs–$Ga_{0.65}Al_{0.35}As$ QWWs at $B = 0$ T. We look at the Ogg–McCombe Hamiltonian; this is an effective Hamiltonian which is diagonal and spin independent at $B = 0$ T. The spin-dependent terms vanish at $B = 0$ T, and therefore the Ogg–McCombe Hamiltonian describes spin-degenerate electron states in the absence of the applied magnetic field. By using an Ogg–McCombe Hamiltonian as a theoretical model in order to calculate the conduction electron effective Landé factor, one needs a spin splitting of the electron states and, therefore, a nonzero applied magnetic field. This is an obvious reason why we have not computed the effective $g_\parallel$ factor at $B = 0$ T. Nevertheless, the present theoretical procedure is useful for studying the magnetic field dependence of the electron $g_\parallel$ factor in semiconductor heterostructures. We have used a logical path in order to support the comparison between our theoretical results at low magnetic fields and the numerical data reported by other authors [5] at $B = 0$ T. First, we have proven that the effective $g_\parallel$ factor depends weakly on the magnetic field at low magnetic field values (cf figure 2). Second, we have shown that our results for low magnetic fields are in good agreement with the theoretical calculations reported by Kiselev *et al* [5] for $B = 0$ T (cf figure 5). In this sense, no important differences between our theoretical results for sufficiently low magnetic-field values and theoretical results at $B = 0$ T obtained by using other numerical procedures are expected to occur.

The good agreement between our theoretical results and those reported in [5] may be understood in terms of the inclusion of remote-band effects, i.e., anisotropy and non-parabolicity of the conduction band in both models. Notice that Kiselev *et al* [5] calculated the electron Landé factor by using an 8×8 Kane model which involves mixing between the lowest conduction band Γ_{6c} and the highest valence bands Γ_{7v} and Γ_{8v}. The present calculation involves non-parabolicity and anisotropy effects being taken into account [16, 18] through the coupling between the lowest Γ_{6c} conduction band, Γ_{7v} and Γ_{8v} valence bands, and the Γ_{7c} and Γ_{8c} p-antibonding conduction bands in GaAs. This leads to a 14×14 Hamiltonian, which may be reduced to a 2×2 conduction-band effective Hamiltonian, i.e., the Ogg–McCombe Hamiltonian [16, 18] (cf equation (1)). In both models the influence of remote bands is taken into account, via a $\vec{\mathbf{k}} \cdot \vec{\mathbf{p}}$ procedure (as in [5]), or by using the effective Ogg–McCombe Hamiltonian, depending on the phenomenological parameters a_i. Therefore one may expect similar results from the two theoretical models. Note that figure 5 also displays the $B = 1$ T effective $g_\parallel$ factor, as a function of the wire radius, disregarding the non-parabolicity and anisotropic terms in the Ogg–McCombe Hamiltonian, i.e., setting the coefficients $a_i = 0$ ($i = 1, 2, 3, \ldots, 6$) in (1) (see the dashed line in figure 5). Previous work on quantum wells [4] has shown that the agreement between theory and experiment is quite poor when anisotropy and non-parabolicity are neglected. Although there are no experimental data against which we can compare, calculations displayed in figure 5 clearly show that the inclusion of these effects substantially changes the calculated $g_\parallel$ factor.

4. Conclusions

Summarizing, we have studied the effects of both the QWW confinement and applied magnetic field on the electron $g_\parallel$ factor in GaAs–$Ga_{1-x}Al_xAs$ cylindrical QWWs. Theoretical calculations were performed by using the Ogg–McCombe effective Hamiltonian which explicitly takes non-parabolicity/anisotropy effects of the conduction band into account. The present theoretical results for the electron $g_\parallel$ factor of GaAs–$Ga_{0.65}Al_{0.35}As$ cylindrical QWWs were found to be in good agreement with previous calculations [5].

Acknowledgments

The authors would like to thank the Colombian COLCIENCIAS Agency, CODI—University of Antioquia, Brazilian Agencies CNPq, FAPESP, the MCT—Institute of the Millennium for Quantum Computing, and Institute of Millennium for Nanotechnology, for partial financial support. LEO wishes to thank for warm hospitality the Institute of Physics of the University of Antioquia, where part of this work was performed.

Appendix

As mentioned before, the expansion (4) is used to solve the Schrödinger equation by turning the differential problem into an algebraic one, i.e., equation (6), which implies a diagonalization of a square matrix with a finite number of elements, with components given by $H_{m_s}^{jk} = \langle\phi_k(\vec{\rho})|\hat{H}_{m_s}|\phi_j(\vec{\rho})\rangle$, and with eigenvalues being the electron-state energies $E_n(m_s)$ obtained for a given projection of the electron spin ($m_s = \uparrow$ or $m_s = \downarrow$) parallel or antiparallel to the applied magnetic field. The number of base functions in the expansion is determined by the acceptable convergence of the eigenvalues. The matrix elements associated with the constant and $\vec{\mathbf{K}}$-dependent terms in $\hat{H}_{m_s}$ may be computed in a relatively easy way, whereas calculations of the matrix elements associated with the electron-confining potential $V(x, y)$ and with the term $\pm\frac{1}{2}g(x, y)\mu_B B$ require a more sophisticated procedure.

For a GaAs–$Ga_{1-x}Al_xAs$ QWW the electron-confining potential is given by

$$V(\vec{\rho}) = \begin{cases} 0 & \text{if } 0 < \rho < R \\ V_0 & \text{if } \rho > R, \end{cases} \tag{A.1}$$

where V_0 is the conduction-potential height. In addition,

$$\tfrac{1}{2}g(\vec{\rho})\mu_B B = \tfrac{1}{2}\mu_B B \begin{cases} g_w & \text{if } 0 < \rho < R \\ g_b & \text{if } \rho > R, \end{cases} \tag{A.2}$$

or, equivalently,

$$\tfrac{1}{2}g(\vec{\rho})\mu_B B = \tfrac{1}{2}g_w\mu_B B + \tfrac{1}{2}\mu_B B \times \begin{cases} 0 & \text{if } 0 < \rho < R \\ g_b - g_w & \text{if } \rho > R, \end{cases} \tag{A.3}$$

where g_w and g_b are the electron Landé factors for GaAs and $Ga_{1-x}Al_xAs$, respectively. The matrix elements of (A.3) are therefore the sums of a diagonal contribution $\frac{1}{2}g_w\mu_B B$ and the matrix elements of a function which depends on the coordinate ρ as the confining potential does.

We have derived a general expression for finding the matrix elements corresponding to an arbitrary function $\mathcal{F} = \mathcal{F}(\rho)$ which is zero in the GaAs cylindrical QWW and takes the finite value $\mathcal{F}_0 \neq 0$ in the $Ga_{1-x}Al_xAs$ barriers, i.e.,

$$\mathcal{F}(\rho) = \begin{cases} 0 & \text{if } 0 < \rho < R \\ \mathcal{F}_0 & \text{if } \rho > R. \end{cases} \tag{A.4}$$

According to (5) the matrix elements of $\mathcal{F}$ are given by

$$\langle\phi_{n_k,l_k}|\mathcal{F}|\phi_{n_{k'},l_{k'}}\rangle = \mathcal{F}_0\delta_{l_k,l_{k'}}\int_{\xi_0}^{+\infty}\xi\, F_{n_k}^{l_k}(\xi)F_{n_{k'}}^{l_k}(\xi)\,\mathrm{d}\xi, \tag{A.5}$$

where $\xi = \frac{\rho}{\sqrt{2}l_B}$, $\xi_0 = \frac{R}{\sqrt{2}l_B}$,

$$F_{n_k}^{l_k}(\xi) = \alpha_{n_k,l_k}\xi^{|l_k|}\mathrm{e}^{-\frac{1}{2}\xi^2}\mathrm{L}_{n_k}^{|l_k|}\left(\xi^2\right), \tag{A.6}$$

and

$$\alpha_{n_k,l_k} = 2\sqrt{\pi}l_B A_{n_k,l_k} = \left[\frac{2n_k!}{(n_k + |l_k|)!}\right]^{\frac{1}{2}}. \tag{A.7}$$

By performing the change of variable $u = \xi^2$ in (A.5) we have

$$\langle\phi_{n_k,l_k}|\mathcal{F}|\phi_{n_{k'},l_{k'}}\rangle = \mathcal{F}_0\delta_{l_k,l_{k'}}I_{n_k,n_{k'}}(l_k, \xi_0, +\infty), \tag{A.8}$$

where

$$I_{n,n'}(l, a, b) = \int_{a^2}^{b^2} f_n^l(u)\, f_{n'}^l(u)\,\mathrm{d}u, \tag{A.9}$$

and

$$f_n^l(u) = \sqrt{\frac{n!}{(n + |l|)!}}u^{\frac{1}{2}|l|}\mathrm{e}^{-\frac{1}{2}u}\mathrm{L}_n^{|l|}(u). \tag{A.10}$$

The expression (A.9) may be solved analytically. After some mathematical manipulations, one may see that the off-diagonal elements ($n \neq n'$) of $I_{n,n'}$ are given by

$$I_{n,n'}(l, a, b) = \frac{1}{n' - n}\Big[\sqrt{n'(n' + |l|)}\, f_n^l(u)\, f_{n'-1}^l(u) - \sqrt{n(n + |l|)}\, f_{n'}^l(u)\, f_{n-1}^l(u) - (n' - n) f_{n'}^l(u) f_n^l(u)\Big]_{a^2}^{b^2}, \tag{A.11}$$

where the artificial condition $f_{-1}^l(u) = 0$, for all values of the real number u and the integer number l, is required in order to appropriately include the cases $n = 0$ or $n' = 0$. For $n = n'$, we have

$$I_{n,n}(l, a, b) = \Big[\frac{2n + |l|}{n}\sqrt{\frac{n}{n + |l|}}\, f_n^l(u)\, f_{n-1}^l(u) - f_n^l(u) f_n^l(u) - f_{n-1}^l(u) f_{n-1}^l(u)\Big]_{a^2}^{b^2} + I_{n-1,n-1}(l, a, b) \tag{A.12}$$

with the initial condition

$$I_{0,0}(l, a, b) = \frac{1}{|l|!}\left[\Gamma\left(|l| + 1, a^2\right) - \Gamma\left(|l| + 1, b^2\right)\right], \tag{A.13}$$

where $\Gamma(x, y)$ is the incomplete Gamma function [19]. According to the formulas (A.11)–(A.13), the matrix elements of $\mathcal{F}$ may be computed through expression (A.8).

References

[1] Oestreich M and Rühle W W 1995 *Phys. Rev. Lett.* **74** 2315
Oestreich M, Hallstein S, Heberle A P, Eberl K, Bauser E and Rühle W W 1996 *Phys. Rev.* B **53** 7911

[2] Hannak R M, Oestreich M, Heberle A P, Ruhle W W and Kohler K 1995 *Solid State Commun.* **93** 313
Le Jeune P, Robart D, Marie X, Amand T, Brosseau M, Barrau J, Kalevich V and Rodichev D 1997 *Semicond. Sci. Technol.* **12** 380
Malinowski A and Harley R T 2000 *Phys. Rev.* B **62** 2051

[3] Pfeffer P and Zawadzki W 2006 *Phys. Rev.* B **74** 233303

[4] de Dios-Leyva M, Reyes-Gómez E, Perdomo-Leiva C A and Oliveira L E 2006 *Phys. Rev.* B **73** 085316
de Dios-Leyva M, Porras-Montenegro N, Brandi H S and Oliveira L E 2006 *J. Appl. Phys.* **99** 104303

[5] Kiselev A A, Ivchenko E L and Rössler U 1998 *Phys. Rev.* B **58** 16353

[6] Notomi M, Hammersberg J, Zeman J, Weman H, Potemski M, Sugiura H and Tamamura T 1998 *Phys. Rev. Lett.* **80** 3125
Danneau R, Klochan O, Clarke W R, Ho L H, Micolich A P, Simmons M Y, Hamilton A R, Pepper M, Ritchie D A and Zülicke U 2006 *Phys. Rev. Lett.* **97** 026403

[7] Medeiros-Ribeiro G, Pinheiro M V B, Pimentel V L and Marega E 2002 *Appl. Phys. Lett.* **80** 4229
Hanson R, Witkamp B, Vandersypen L M K, Willems van Beveren L H, Ellerman J M and Kouwenhoven L P 2003 *Phys. Rev. Lett.* **91** 196802
Pryor C E and Flatté M E 2006 *Phys. Rev. Lett.* **96** 026804
Mayer Alegre T P, Hernández F G G, Pereira A L C and Medeiros-Ribeiro G 2006 *Phys. Rev. Lett.* **97** 236402

[8] Reyes-Gómez E, Perdomo-Leiva C A, de Dios-Leyva M and Oliveira L E 2006 *Phys. Rev.* B **74** 033314

[9] Kato Y K, Myers R C, Gossard A C and Awschalom D D 2004 *Science* **306** 1910
Zutic I, Fabian J and Das Sarma S 2004 *Rev. Mod. Phys.* **76** 323
Chen Z, Carter S G, Bratschitsch R, Dawson P and Cundiff S T 2007 *Nat. Phys.* **3** 265

[10] Liang C-T, Cheng Y-M, Huang T Y, Huang C F, Simmons M Y, Ritchie D A, Kim G-H, Leem J Y, Chang Y H and Chen Y F 2001 *J. Phys. Chem. Solids* **62** 1789

[11] Leadley D R, Nicholas R J, Maude D K, Utjuzh A N, Portal J C, Harris J J and Foxon C T 1997 *Phys. Rev. Lett.* **79** 4246

[12] Leadley D R, Nicholas R J, Maude D K, Utjuzh A N, Portal J C, Harris J J and Foxon C T 1998 *Semicond. Sci. Technol.* **13** 671

[13] Li Y, Qian F, Xiang J and Lieber C M 2006 *Mater. Today* **9** 18

[14] Ogg N R 1966 *Proc. Phys. Soc.* **89** 431
McCombe B O 1969 *Phys. Rev.* **181** 1206

[15] Li E H 2000 *Physica* E **5** 215

[16] Golubev V G, Ivanov-Omskiĭ V I, Minervin I G, Osutin A V and Polyakov D G 1985 *Sov. Phys.—JETP* **61** 1214

[17] Bronold F X, Martin I, Saxena A and Smith D L 2002 *Phys. Rev.* B **66** 233206

[18] Braun M and Rössler U 1985 *J. Phys. C: Solid State Phys.* **18** 3365
Lommer G, Malcher F and Rössler U 1985 *Phys. Rev.* B **32** 6965
Malcher F, Lommer G and Rössler U 1986 *Superlattices Microstruct.* **2** 267
Lommer G, Malcher F and Rössler U 1986 *Superlattices Microstruct.* **2** 273

[19] Abramowitz M and Stegun I A (ed) 1964 *Handbook of Mathematical Functions* (New York: Dover)